ChemPubSoc Europe

DOI: 10.1002/ejoc.201600005

EurJOC European Journal of Organic Chemistry

Full Paper

Heteroacene Synthesis

Mechanochemical Synthesis, Photophysical Properties, and X-ray Structures of N-Heteroacenes

Prasit Kumar Sahoo,[a] Chandan Giri,[a,b] Tuhin Subhra Haldar,[a] Rakesh Puttreddy,[b] Kari Rissanen*[b] and Prasenjit Mal*[a]

Abstract: The described mechanochemical methodology is an example of a proof-of-concept in which solution-based tedious, poor yielding, and difficult syntheses of pyrazaacenes are achieved under solvent-free ball-milling conditions; the method is easy, high yielding, time-efficient, and environmentally benign. The synthesized compounds also include pyrazaacenes (N-heteroacenes) that are octacene analogues containing pyrene building blocks. The compounds were sparingly soluble in common solvents, and column chromatographic purifications could be avoided after the solvent-free syntheses. The UV/Vis absorption spectra of the pyrazaacenes show intense absorption bands in the near-IR region. The single-crystal X-ray analyses of selected pyrazaacene derivatives showed pairwise π–π interactions and some C–H···π interactions, which could account for some of the photophysical features of the compounds in the solid state.

Introduction

The recent advances in the syntheses of extended π-conjugated acene molecules with exciting optoelectronic properties have led to significant interest in these compounds for materials science.[1] Generally, acenes are considered as the most comprehensive class of fused polycyclic aromatic hydrocarbons and are described by the fewest localized Clar resonant sextets per number of aromatic rings.[2] The uses of these materials vary from moth repellents to precursors for synthetic dyes such as alizarin. Also, owing to their electronic properties, these molecules have gained attention for applications such as field-effect transistors (FETs), organic light-emitting diodes (OLEDs), and photovoltaic cells. Unfortunately, acenes are highly unstable, and the incorporation of heteroatoms increases their stability.[3] These heteroacenes display improved stability compared to their hydrocarbon analogues because it is much easier to make C–N bonds than C–C bonds.[4] Owing to their electron-deficient nature, small band gaps, and high thermal stabilities, heteroacenes are considered to be alternatives to acenes as potential n-type semiconducting materials.[1d,3]

Herein, we mainly focus our attention on the synthesis of pyrazaacenes or N-heteroacenes, that is, nitrogen-containing heteroacenes with either pyrene building blocks or pyrene-fused oligoazaacenes. In general, N-heteroacenes are synthesized by two popular methods: (1) cyclocondensation reactions between 1,2-diaminoarenes and 1,2-diketones;[5] (2) substitution reactions of 1,2-diaminoarenes with dihydroxyacenes, followed by oxidation.[3,4] However, these pyrazaacenes are synthesized by following the cyclocondensation method, because –C=N bonds are readily constructed through this reaction.[5b] The major disadvantages of the known syntheses of pyrazaacenes are associated with the hazardous reaction conditions and low yields; therefore, very few methods are available for pyrazaacene synthesis.[5a,6]

Recently, as result of public interest in alternative energy input,[7] ball-milling mechanochemistry[8] has received significant interest from chemists as a solvent-free synthetic methodology owing to its benefits over traditional solution-based methods.[9] The advantages of mechanochemistry are substantial and well-documented.[7] This technique has huge significance to green processes and is time efficient, environmentally benign, and economical. The minimum purification required, quantitative conversions, and the production of fewer byproducts bring extra importance to this method. Under the area of mechanochemistry, we have recently reported multistep syntheses,[10] metal-free synthetic methodologies,[11] and self-sorting reactions.[12] Therefore, we have anticipated that solvent-free synthesis by the ball-milling methodology may possibly be used as a supply of mechanical energy and that reactions for the synthesis of heteroacenes could be performed in a greener way.[13] Taking into consideration all of these aspects, we have designed a straightforward mechanochemical route for the

[a] School of Chemical Sciences, National Institute of Science Education and Research (NISER) Bhubaneswar,
PO Bhimpur-Padanpur, Via Jatni, District Khurda, Odisha 752050, India
E-mail: pmal@niser.ac.in
http://www.niser.ac.in/users/pmal

[b] University of Jyvaskyla, Department of Chemistry, Nanoscience Center,
P. O. Box. 35, 40014 University of Jyvaskyla, Finland
E-mail: kari.t.rissanen@jyu.fi
https://www.jyu.fi/kemia/tutkimus/orgaaninen/en/research/rissanen

Supporting information and ORCID(s) from the author(s) for this article are available on the WWW under http://dx.doi.org/10.1002/ejoc.201600005.

preparation of N-heteroacenes in a limited number of synthetic steps, under solvent-free conditions, and in high yields.

Results and Discussion

Synthesis

The mechanochemical (ball-milling) syntheses of heteroacenes from their respective precursors are outlined in Figure 1. 1,2-Dicarbonyl compounds (**1**) and 1,2-diaminoarenes (**2**) were used as precursors for the solvent-free cyclocondensation reactions. The reactions were performed under ambient laboratory conditions with *p*-toluenesulfonic acid (PTSA) as the catalyst. For optimization, the reaction progress was monitored by thin layer chromatography (TLC) or ^{1}H NMR spectroscopy. As a standard method, the milling instrument was stopped, and a small sample was collected from the reaction jar and analyzed. After the reactions were complete, the solid products were collected in a flask, washed with an appropriate solvent, and collected by filtration. The substrate scope of this methodology was verified, and the results are shown in Figure 2.

As shown in Figure 2 (a), excellent yields (91–95 %) of pyrazaacene derivatives were obtained from pyrene-4,5-dione (**1a**)[14] and different diamines. Similar high-yielding reactions were observed for the synthesis of pyrazaacene derivatives from other dicarbonyl or tetracarbonyl derivatives (Figure 2, b–d). In the majority of cases, a single product was obtained; therefore, purification by washing with an appropriate solvent (mainly highly polar solvents) led to the isolation of analytically pure products (Figure 3, ^{1}H NMR spectra). By this methodology, we also synthesized the octacene derivatives benzo[*i*]benzo[6′,7′]-quinoxalino[2′,3′:9,10]phenanthro[4,5-*abc*]phenazine (**3bb**)[15] and 2,13-di-*tert*-butylbenzo[*i*]benzo[6′,7′]quinoxalino[2′,3′:9,10]-

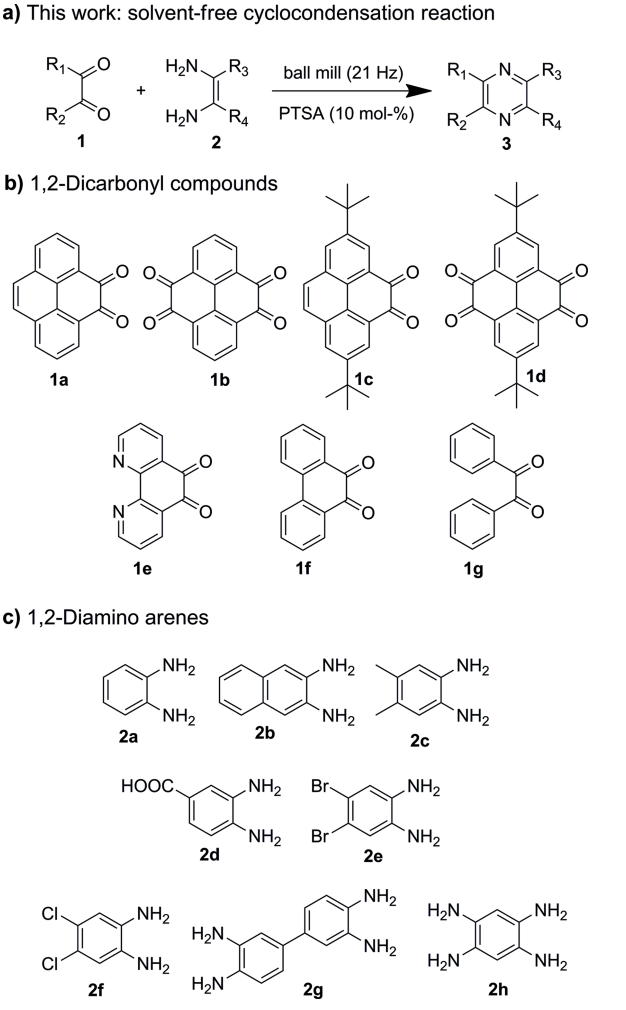

Figure 1. Mechanochemical approach for heteroacene synthesis.

Table 1. Efficiency of the synthesis by ball milling.

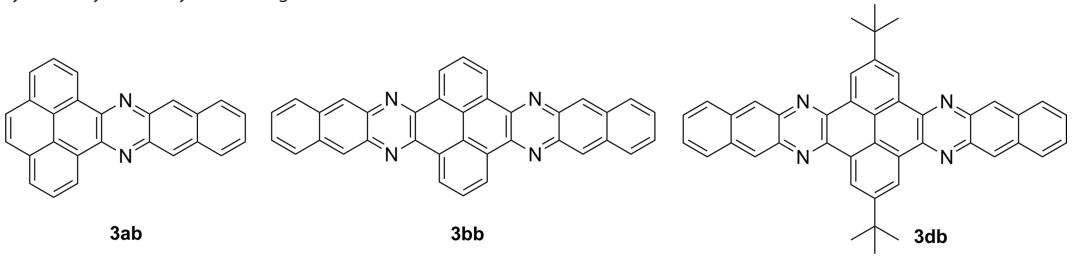

Entry		Information	Previous work	This work
1	**3ab**	method:	ref.[16]	ball mill
		reaction conditions:	pyridine, reflux, Ar atm, 3 d	r.t., 3 h, PTSA catalyst
		isolation procedure:	workup and then flash chromatography	solid residue washed with ethanol
		yield [%]	32	95
2	**3bb**	method:	ref.[17]	ball mill
		reaction conditions:	pyridine, 120 °C, Ar atm, 3 d	r.t., 4 h, PTSA catalyst
		isolation procedure:	solid residue washed with ethanol and then chloroform	solid residue washed with ethanol and then DMF
		yield [%]	40	78
3	**3db**	method:	ref.[5a]	ball mill
		reaction conditions:	pyridine, 120 °C, Ar atm, 3 d	r.t., 4 h, PTSA catalyst
		isolation procedure:	solid residue washed with ethanol and chloroform	solid residue washed with ethanol and then DMF
		yield [%]	32	76

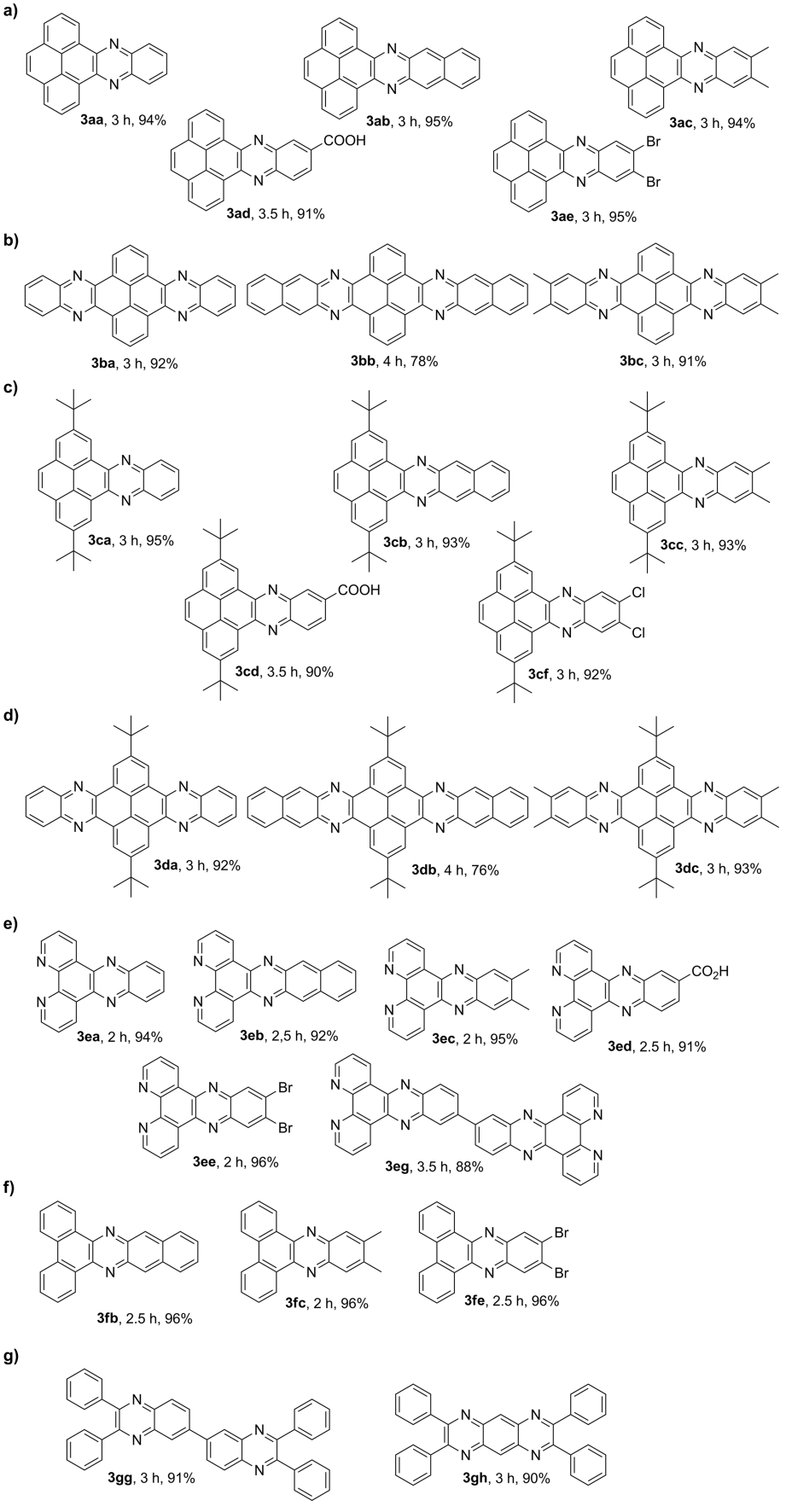

Figure 2. The mechanochemically synthesized N-heteroacenes are shown with their compound identification numbers, reaction times, and isolated yields.

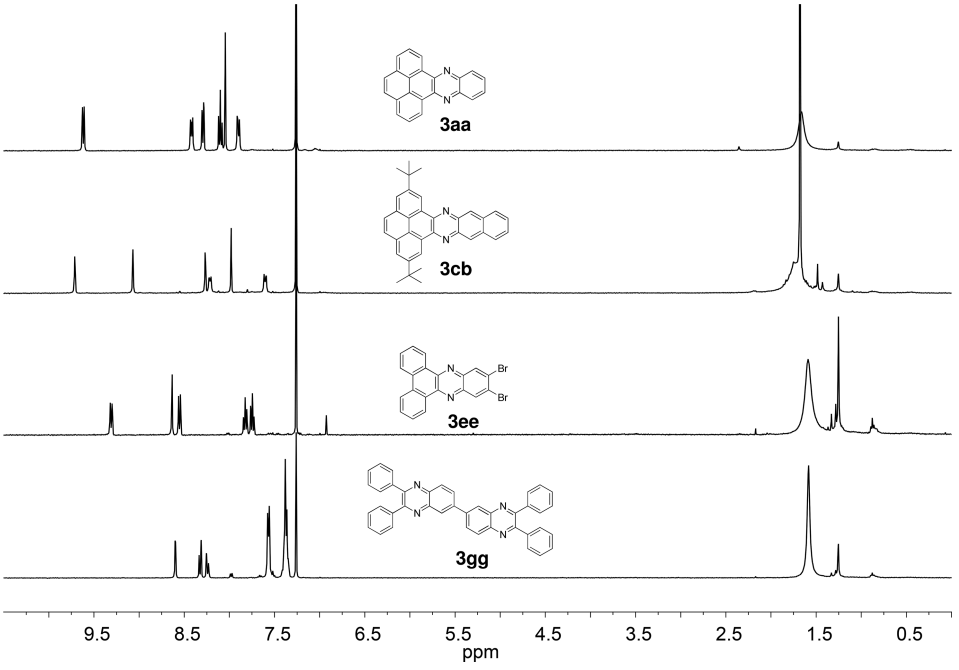

Figure 3. ^{1}H NMR spectra of **3aa**, **3cb**, **3ee**, and **3gg** in $CDCl_3$. No purifications of these compounds were performed before the spectra were recorded.

phenanthro[4,5-*abc*]phenazine (**3db**) in good yields. The octacenes (**3bb** and **3db**) were purified by washing with highly polar solvents such as *N*,*N*-dimethylformamide (DMF).

As pyrazine is one of the most important heterocyclic cores in heteroacene systems, we extended our methodology to other classes of N-heteroacene analogues. By using different 1,2-diketones (Figure 1, b) such as benzil (**1g**), 1,10-phenanthroline-5,6-dione (**1e**), and phenanthrene-5,6-dione (**1f**), we synthesized different classes of N-heteroacenes in excellent yields (Figure 2, e–g). Similarly, the bis(phenazine) **3eg** and the bis(quinoxaline) **3gg** were also obtained in excellent yields (ca. 90 %) from (1,1′-biphenyl)-3,3′,4,4′-tetraamine (**2g**) and benzene-1,2,4,5-tetraamine (**2h**), respectively.

The commonly used methods to synthesize pyrazine-containing heteroacenes use ethanol/acetic acid or acetic acid under reflux in the presence of the oxidant 2-iodoxybenzoic acid (IBX). In all of these cases, the reaction conditions are hazardous, time consuming, and often lead to very poor yields. Interestingly, this method is simple, convenient, time-efficient, economical, and environmentally friendly. A comparison of the syntheses of a few heteroacenes by our method and by literature methods is presented in Table 1. Hence, it is established that our methodology for the synthesis of heteroacenes is superior to the existing ones.

^{1}H NMR Spectroscopy

The solvent-free syntheses were performed under ambient conditions, and ^{1}H NMR spectroscopy studies helped us to understand the efficiency of this described methodology. No chromatographic purifications were performed; however, by washing the products with minimum quantities of highly polar solvents, the compounds were isolated with high purity for further studies. As representative examples, the ^{1}H NMR spectra of **3aa**, **3cb**, **3ee**, and **3gg** without any purification are shown in Figure 3. Thus, the efficiency of this ball-mill method for the synthesis of N-heteroacenes has been established.

Photophysical Study[18]

The absorption and photoluminescence spectra of the compounds were recorded in appropriate solvents, and selective data are shown in Table 2. The absorption maxima of the compounds above λ = 400 nm are due to n–π^* transitions. As expected, with increasing conjugation, more redshifted absorptions were observed, for example, $\lambda_{max} \approx$ 435 nm for **3aa** and 469 nm for **3ab**. The UV/Vis absorption spectra of pyrazaacenes **3aa**–**3ae** in dichloromethane are shown in Figure 4.

Table 2. Absorption maxima, emission maxima, and fluorescence quantum yields for selected compounds.

	λ_{abs} [nm]	λ_{em} [nm]	Φ
3aa	435	471	0.35
3ab	469	502	0.16
3ac	434	462	0.47
3ad	447	490	0.12
3ae	452	494	0.02
3ca	439	480	0.42
3cb	474	511	0.17
3cc	438	471	0.48
3cd	455	507	0.32
3cf	456	503	0.08
3ba	412	442	0.10
3bc	417	446	0.23
3da	415	443	0.11
3dc	419	440	0.28

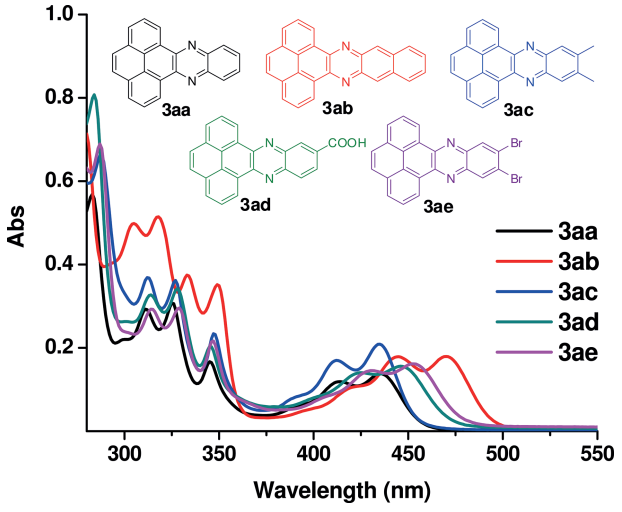

Figure 4. UV/Vis absorption spectra of pyrazaacenes **3aa**–**3ae** in dichloromethane (1×10^{-5} M).

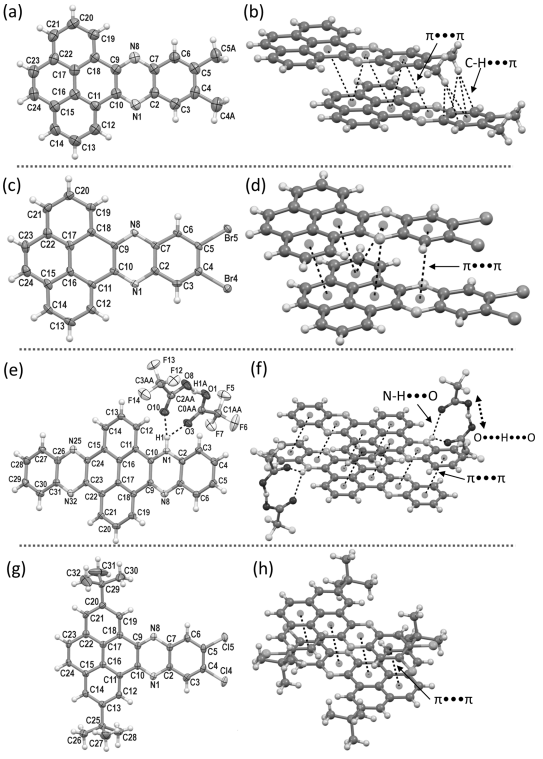

Figure 5. Left: X-ray crystal structures of (a) **3ac**, (c) **3ae**, (e) **3ba**, and (g) **3cf** with thermal ellipsoids at 50 % probability level. Hydrogen atoms are not labeled for clarity. Right: the corresponding motifs showing π–π interactions.

Crystallographic Investigations

The molecular structures of polycyclic aromatic hydrocarbons (PAHs) are not very interesting.[1e] However, heteroatom-containing PAHs and their solid-state organizational features such as enhanced π–π interactions are very interesting and can be understand through X-ray crystallography.[19] In the solid-state, the extent of π–π and C–H•••π interactions in N-heteroacenes are believed to be further improved by the substituents and any π disturbances caused by the inclusion of charged species. These concepts are explored within the crystal structures of **3ac**, **3ae**, **3ba**, and **3cf**, as are the forces that drive the association of the aromatic rings through π–π and C–H•••π interactions.[18,20]

All of the crystal structures show characteristic π–π interactions, as shown in Figure 5. Compound **3ac** displays a herringbone pattern (Figure S45) with the aromatic rings displaced laterally and stabilized by pairwise π–π interactions at centroid-to-centroid distances of 3.562 to 3.786 Å. Additionally, the lateral displacement allows the methyl substituents to form C–H•••π interactions (ca. 2.780 to 3.022 Å), as shown in Figure 5 (b). In **3ae**, the aromatic rings are displaced such that the bromine-substituted benzene ring stacks uniquely above the pyrazine ring stabilized by pairwise π–π interactions (ca. 3.532 to 3.849 Å), as shown in Figure 5 (d). The packing of **3ae** is influenced by the bromine substituents and again displays a herringbone solid-state organization stabilized by π–π and Br•••Br interactions (ca. 3.602 Å). All of the interatomic distances in the crystal-packing interactions are shorter than the sum of the van der Waals radii (Figure S46).

As shown in Figure 5 (f), **3ba** clearly has the most-abundant and efficient π–π interactions (ca. 3.608 to 3.808 Å) of all of the compounds. This can be accounted for by the protonation of a pyrazine nitrogen atom. The N–H moiety acts as a bifurcated hydrogen-bond donor for two trifluoroacetate C–O oxygen atoms with slight double-bond character [1.211(3) Å] at distances of 2.726(3) [angle N–H•••O 144°] and 2.802(3) Å [angle N–H•••O 115°]. On the other hand, the C–O oxygen atoms [1.273(3) Å] of the trifluoroacetate anions are further stabilized by unsymmetrical O•••H•••O hydrogen bonds with distances of 1.21(5) and 1.23(4) Å [angle O•••H•••O 167(4)°], as shown in Figure 5 (f). The crystal packing is further extended one-dimensionally by π–π interactions (ca. 3.737 Å) and two dimensionally by weak C–H•••O interactions between the trifluoroacetate anions and the hydrogen atoms of the aromatic rings to generate herringbone (viewed along the *a* axis) and sinusoidal (viewed along the *c* axis) patterns (Figure S46). Although the C–H•••O interactions deviate by 0.122 Å from the sum of the van der Waals radii and are caused by the packing, they are important in the crystal-packing stabilization. The efficient π-cloud delocalization between the pyrene core with electron-donating *tert*-butyl-substituted and pyrazine-fused benzene rings with electron-withdrawing chloride substituents results in strong π–π interactions in **3cf**. The π–π interactions occur one-dimensionally without aromatic-ring displacements (Figure S47) but in an inverted fashion to avoid steric hindrance between the *tert*-butyl groups, as shown in Figure 5 (h). The centroid-to-centroid distances range from 3.415 to 3.698 Å. The crystal packing of **3cf** is trivial, and all of the observed C–H•••π interactions are above the sum of the van der Waals radii. The Hirshfeld surface plots and 2D fingerprint analyses are given in the Supporting Information.

Conclusions

We foresee that the benefits of the mechanochemical synthesis of the pyrazaacenes will be substantial: (a) this could potentially

be the most efficient approach for heteroacene synthesis; (b) the room-temperature synthesis, shorter reaction time, and simplified purification procedure will make the heteroacenes cheaply available for materials chemistry applications. The X-ray crystal analysis of a few pyrazaacene derivatives show pairwise π–π interactions and some C–H···π interactions, which may result in conductivity properties in the solid state. We are exploring the conducting behavior of the N-heteroacenes. Further, we anticipate that our study may receive substantial attention from researchers working on the development of synthetic methodologies with N-heteroacenes as well as chemists searching for superior methods in organic mechanochemistry.

Experimental Section

General Methods: Ball-mill syntheses (21 Hz) were performed in the open atmosphere with a Retsch MM 200 mixer mill in a 10 mL ZrO_2 or stainless-steel jar with one ball of 15 mm diameter made of ZrO_2 or stainless-steel, respectively. The NMR spectra were recorded with a 400 MHz instrument at 25 °C. The chemical shift values are reported in parts per million (ppm) and were referenced to the residual chloroform (δ = 7.26 ppm for ^{1}H, δ = 77.16 ppm for ^{13}C) and deuterium oxide signals (δ = 4.79 ppm for ^{1}H). The peak patterns are designated as follows: s singlet, d doublet, t triplet, q quartet, m multiplet, dd doublet of doublets, td triplet of doublets, br. s broad singlet. The coupling constants (*J*) are reported in Hertz (Hz). High-resolution mass spectrometry (HRMS) was conducted with an ESI-TOF mass spectrometer. The infrared spectroscopic data are reported in wavenumbers (cm^{-1}). The melting points of the compounds were determined with a digital melting point apparatus.

Phenanthro[4,5-*abc*]phenazine (3aa): Pyrene-4,5-dione (**1a**, 50 mg, 0.21 mmol), *o*-phenylenediamine (**2a**, 23 mg, 0. 21 mmol), PTSA (4 mg, 0.021 mmol), and a stainless-steel ball were added to a stainless-steel jar (10 mL). Milling was performed for 3 h, after which the crude reaction mixture was washed with ethanol to isolate the product as yellowish solid; yield 94 % (62 mg); m.p. 257–259 °C (ref.[21] 276.8–277.4 °C). ^{1}H NMR (400 MHz, $CDCl_3$): δ = 9.59 (dd, *J* = 7.7, 0.9 Hz, 2 H), 8.39 (dd, *J* = 6.5, 3.4 Hz, 2 H), 8.28 (dd, *J* = 7.7, 0.9 Hz, 2 H), 8.10 (t, *J* = 7.7 Hz, 2 H), 8.03 (s, 2 H), 7.90 (dd, *J* = 6.5, 3.4 Hz, 2 H) ppm. ^{13}C NMR (100 MHz, $CDCl_3$): δ = 143.5, 142.6, 131.6, 130.1, 129.7, 129.7, 129.4, 127.4, 127.0, 126.3, 124 ppm. IR (KBr): $\tilde{\nu}$ = 3049, 2923, 1624, 1480, 1422, 1359, 1334, 1314, 1292, 1174, 1094, 1063, 830, 763, 713, 630, 587, 426 cm^{-1}. HRMS: calcd. for $C_{22}H_{12}N_2$ [M + H]$^+$ 305.1073; found 305.1088.

Large-Scale Synthesis: The suggested loading of the reactants is less than one third of the jar volume (25 mL ZrO_2 jar). Compound **3aa** was also synthesized from pyrene-4,5-dione (1.2 g), *o*-phenylenediamine (552 mg), and PTSA (96 mg), yield 1.5 g (94 %).

Benzo[*i*]phenanthro[4,5-*abc*]phenazine (3ab):[16] Yellow solid; yield 95 % (72 mg); m.p. >300 °C. ^{1}H NMR (400 MHz, CF_3CO_2D): δ = 9.62 (d, *J* = 7.6 Hz, 2 H), 9.25 (d, *J* = 3.2 Hz, 2 H), 8.73 (d, *J* = 7.7 Hz, 2 H), 8.52 (dd, *J* = 6.3, 3.1 Hz, 2 H), 8.48 (t, *J* = 7.7 Hz, 2 H), 8.30 (d, *J* = 2.3 Hz, 2 H), 8.17 (dd, *J* = 6.5, 2.9 Hz, 2 H) ppm. ^{13}C NMR (101 MHz, CF_3CO_2H): δ = 142.0, 138.1, 136.4, 134.2, 133.1, 132.5, 130.2, 130.1, 129.8, 127.5, 127.3, 125.4, 124.1 ppm. IR (KBr): $\tilde{\nu}$ = 3049, 2917, 1855, 1624, 1421, 1358, 1294, 1262, 1176, 1098, 874, 829, 737, 716, 486 cm^{-1}. HRMS: calcd. for $C_{26}H_{14}N_2$ [M + H]$^+$ 355.1230; found 355.1241.

11,12-Dimethylphenanthro[4,5-*abc*]phenazine (3ac): Pale orange solid; yield 94 % (67 mg); m.p. 238–240 °C. ^{1}H NMR (400 MHz, $CDCl_3$): δ = 9.54 (d, *J* = 7.7 Hz, 2 H), 8.26 (d, *J* = 7.7 Hz, 2 H), 8.08–8.05 (m, 4 H), 8.02 (s, 2 H), 2.58 (s, 6 H) ppm. ^{13}C NMR (100 MHz, $CDCl_3$): δ = 142.6, 141.7, 140.9, 131.6, 130.0, 128.9, 128.5, 127.3, 126.9, 126.1, 123.7, 20.7 ppm. IR (KBr): $\tilde{\nu}$ = 3041, 2920, 2848, 1613, 1354, 1295, 1096, 1001, 867, 831, 719, 438 cm^{-1}. HRMS: calcd. for $C_{24}H_{16}N_2$ [M + H]$^+$ 333.1386; found 333.1410.

Phenanthro[4,5-*abc*]phenazine-11-carboxylic Acid (3ad): Orange solid; yield 91 % (68 mg); m.p. 246–248 °C. ^{1}H NMR (400 MHz, $CDCl_3$): δ = 9.57 (s, 2 H), 9.41 (s, 1 H), 8.80 (s, 2 H), 8.60 (dd, *J* = 22.0, 6.9 Hz, 2 H), 8.25 (s, 2 H), 8.19 (q, *J* = 9.3 Hz, 2 H) ppm. ^{13}C NMR (100 MHz, $CDCl_3$): δ = 170.0, 144.68, 140.7, 138.4, 136.0, 135.8, 134.5, 134.4, 133.2, 132.6, 132.4, 131.0, 128.9, 128.8, 128.7, 128.2, 127.5, 127.4, 126.5, 126.4, 124.8, 124.3, 121.8 ppm. IR (KBr): $\tilde{\nu}$ = 3050, 2880, 1688, 1680, 1435, 1358, 1283, 1206, 1134, 1023, 832, 801, 714 cm^{-1}. HRMS: calcd. for $C_{23}H_{12}N_2O_2$ [M + H]$^+$ 349.0972; found 349.0993.

11,12-Dibromophenanthro[4,5-*abc*]phenazine (3ae): Yellow solid; yield 95 % (85 mg); m.p. >300 °C. ^{1}H NMR (400 MHz, $CDCl_3$): δ = 9.43 (s, 2 H), 8.87 (s, 2 H), 8.50 (d, *J* = 6.5 Hz, 2 H), 8.18 (s, 2 H), 8.10 (s, 2 H) ppm. ^{13}C NMR (100 MHz, $CDCl_3$): δ = 141.8, 136.0, 134.0, 132.2, 132.1, 129.9, 128.5, 128.2, 126.5 126.4, 123.8 ppm. IR (KBr): $\tilde{\nu}$ = 3063, 3046, 2917, 2843, 1624, 1442, 1353, 1293, 1171, 1099, 1080, 903, 833, 714, 434 cm^{-1}. HRMS: calcd. for $C_{22}H_{10}Br_2N_2$ [M + H]$^+$ 460.9283; found 460.9253.

Quinoxalino[2′,3′:9,10]phenanthro[4,5-*abc*]phenazine (3ba): Pale yellow solid; yield 92 % (71 mg); m.p. >300 °C (ref.[22] >420 °C). ^{1}H NMR (400 MHz, $CDCl_3$): δ = 9.98 (d, *J* = 8.0 Hz, 4 H), 8.79 (dd, *J* = 6.4, 3.3 Hz, 4 H), 8.59 (t, *J* = 8.0 Hz, 2 H), 8.40 (dd, *J* = 6.5, 3.1 Hz, 4 H) ppm. ^{13}C NMR (100 MHz, $CDCl_3$): δ = 130.0, 137.7, 136.4, 132.1, 131.0, 128.9, 126.1, 125.2 ppm. IR (KBr): $\tilde{\nu}$ = 3053, 3011, 2923, 1957, 1903, 1613, 1479, 1415, 1403, 1356, 1332, 1294, 1231, 1133, 1101, 976, 870, 809, 759, 720, 615, 570, 515, 443 cm^{-1}. HRMS: calcd. for $C_{28}H_{14}N_4$ [M + H]$^+$ 407.1291; found 407.1290.

Benzo[*i*]benzo[6′,7′]quinoxalino[2′,3′:9,10]phenanthro[4,5-*abc*]-phenazine (3bb):[17] Orange solid; yield 78 % (71 mg); m.p. >300 °C. ^{1}H NMR (400 MHz, CF_3CO_2D): δ = 9.19 (d, *J* = 8.0 Hz, 4 H), 8.52 (s, 4 H), 7.19 (t, *J* = 8.0 Hz, 2 H), 7.58 (m, 4 H), 7.13 (m, 4 H) ppm. IR (KBr): $\tilde{\nu}$ = 3428, 2338, 1677, 1406, 1359, 1327, 1298, 1207, 1178, 1132, 1094, 1022, 897, 869, 805, 774, 721 cm^{-1}. The HRMS data could not be obtained owing to the insoluble nature of the compound.

6,7,15,16-Tetramethylquinoxalino[2′,3′:9,10]phenanthro[4,5-*abc*]phenazine (3bc): Yellow solid; yield 91 % (80 mg); m.p. >300 °C (ref.[22] >420 °C). ^{1}H NMR (400 MHz, $CDCl_3$): δ = 9.91 (d, *J* = 8.0 Hz, 4 H), 8.54 (t, *J* = 8.0 Hz, 2 H), 8.50 (s, 4 H), 2.78 (s, 12 H) ppm. ^{13}C NMR (101 MHz, $CDCl_3$): δ = 149.6, 137.6, 137.0, 131.0, 130.6, 128.1, 125.2, 124.6, 21.5 ppm. IR (KBr): $\tilde{\nu}$ = 2976, 2915, 1621, 1474, 1449, 1397, 1353, 1338, 1215, 1112, 1027, 998, 066, 894, 815, 723, 445 cm^{-1}. HRMS: calcd. for $C_{32}H_{22}N_4$ [M + H]$^+$ 463.1917; found 463.1916.

2,7-Di-*tert*-butylphenanthro[4,5-*abc*]phenazine (3ca): Yellow solid; yield 95 % (57 mg); m.p. >300 °C. ^{1}H NMR (400 MHz, $CDCl_3$): δ = 9.69 (d, *J* = 4.0 Hz, 2 H), 8.44 (q, *J* = 4.0 Hz, 2 H), 8.28 (d, *J* = 4.0 Hz, 2 H), 8.00 (s, 2 H), 7.89 (q, *J* = 4.0 Hz, 2 H), 1.67 (s, 18 H) ppm. ^{13}C NMR (101 MHz, $CDCl_3$): δ = 149.9, 144.1, 131.4, 129.8, 129.7, 129.2, 127.5, 126.0, 124.5, 121.7, 35.7, 32.1 ppm. IR (KBr): $\tilde{\nu}$ = 2961, 2885, 2867, 2333, 1815, 1759, 1612, 1625, 1610, 1477, 1438, 1364, 1353, 1346, 1328, 1259, 1201, 1169, 1112, 1033, 972, 948, 912,

887, 803, 760, 723, 582 cm^{-1}. HRMS: calcd. for $C_{30}H_{28}N_2$ $[M + H]^+$ 417.2325; found 417.2355.

2,7-Di-*tert*-butylbenzo[*i*]phenanthro[4,5-*abc*]phenazine (3cb): Yellow solid; yield 93 % (63 mg); m.p. >300 °C. ^1H NMR (400 MHz, $CDCl_3$): δ = 9.70 (d, J = 4.0 Hz, 2 H), 9.03 (s, 2 H) 8.28 (d, J = 4.0 Hz, 2 H), 8.24 (m, 2 H), 8.00 (s, 2 H), 7.63 (m, 2 H), 1.69 (s, 18 H) ppm. ^{13}C NMR (101 MHz, $CDCl_3$): δ = 150.1, 145.3, 139.1, 134.2, 121.5, 129.3, 128.8, 127.7, 127.4, 126.7, 126.6, 124.7, 122.3, 35.7, 32.1 ppm. IR (KBr): $\tilde{\nu}$ = 3051, 2866, 2743, 2713, 2689, 2668, 2485, 2333, 2324, 1625, 1612, 1552, 1480, 1474, 1436, 1390, 1365, 1344, 1283, 1257, 1236, 1201, 1161, 1109, 1098, 975, 948, 890, 803, 739, 723, 601, 616, 578 cm^{-1}. HRMS: calcd. for $C_{34}H_{30}N_2$ $[M + H]^+$ 467.2482; found 467.2509.

2,7-Di-*tert*-butyl-11,12-dimethylphenanthro[4,5-*abc*]phenazine (3cc): Yellow solid; yield 93 % (60 mg); m.p. >300 °C. ^1H NMR (400 MHz, $CDCl_3$): δ = 9.64 (d, J = 4.0 Hz, 2 H), 8.25 (d, J = 4.0 Hz, 2 H), 8.17 (s, 2 H), 7.99 (s, 2 H), 2.62 (s, 6 H), 1.66 (s, 18 H) ppm. ^{13}C NMR (101 MHz, $CDCl_3$): δ = 149.7, 143.2, 141.5, 140.6, 131.3, 129.5, 128.5, 127.4, 125.6, 124.3, 121.3, 35.7, 32.1, 20.7 ppm. IR (KBr): $\tilde{\nu}$ = 2963, 2868, 2331, 1625, 1612, 1509, 1479, 1444, 1363, 1346, 1327, 1262, 1242, 1225, 1209, 1161, 1123, 1057, 1033, 1000, 964, 887, 866, 804, 724, 624, 601, 577 cm^{-1}. HRMS: calcd. for $C_{34}H_{30}N_2$ $[M + H]^+$ 445.2638; found 445.2699.

2,7-Di-*tert*-butylphenanthro[4,5-*abc*]phenazine-11-carboxylic Acid (3cd): Yellow solid; yield 90 % (61 mg); m.p. >300 °C. ^1H NMR (400 MHz, $CDCl_3$): δ = 9.63 (s, 1 H), 9.53 (s, 1 H), 9.42 (s, 1 H), 8.79 (d, J = 8.0 Hz, 1 H), 8.72 (d, J = 8.0 Hz, 1 H), 8.59 (s, 1 H), 8.53 (s, 1 H), 8.15 (m, 2 H), 1.66 (s, 9 H), 1.62 (s, 9 H) ppm. ^{13}C NMR (101 MHz, $CDCl_3$): δ = 152.5, 152.3, 145.3, 141.3, 138.1, 135.6, 134.1, 133.0, 132.8, 132.3, 132.2, 131.0, 130.9, 128.7, 128.2, 125.9, 124.9, 124.6, 124.4, 124.2, 124.0, 36.0, 31.7, 31.5 ppm. IR (KBr): $\tilde{\nu}$ = 2661, 2551, 1845, 1690, 1616, 1486, 1442, 1363, 1344, 1302, 1283, 1261, 1226, 1166, 978, 887, 843, 795, 767, 722, 554 cm^{-1}. HRMS: calcd. for $C_{31}H_{28}N_2O_2$ $[M + H]^+$ 461.2224; found 461.2249.

2,7-Di-*tert*-butyl-11,12-dichlorophenanthro[4,5-*abc*]phenazine (3cf): Yellow solid; yield 92 % (65 mg); m.p. >300 °C. ^1H NMR (400 MHz, $CDCl_3$): δ = 9.59 (d, J = 4.0 Hz, 2 H), 8.53 (s, 2 H), 8.31 (d, J = 4.0 Hz, 2 H), 8.01 (s, 2 H), 1.67 (s, 18 H) ppm. ^{13}C NMR (101 MHz, $CDCl_3$): δ = 152.5, 142.4, 140.6, 134.7, 132.4, 131.9, 128.5, 125.9, 125.2, 124.1, 122.7, 36.0, 31.5 ppm. IR (KBr): $\tilde{\nu}$ = 2958, 2884, 2866, 1906, 1820, 1810, 1799, 1787, 1759, 1752, 1729, 1610, 1593 1473, 1449, 1406, 1383, 1364, 1330, 1287, 1240, 1219, 1171, 1127, 1111, 1103, 986, 888, 866, 798, 722, 528 cm^{-1}. HRMS: calcd. for $C_{34}H_{30}N_2$ $[M + H]^+$ 485.1546; found 485.1526.

2,11-Di-*tert*-butylquinoxalino[2′,3′:9,10]phenanthro[4,5-*abc*]-phenazine (3da):[23] Pale yellow solid; yield 92 % (64 mg); m.p. >300 °C (ref. >300 °C). ^1H NMR (400 MHz, $CDCl_3$): δ = 9.94 (s, 4 H), 8.77 (m, 4 H), 8.39 (m, 4 H), 1.71 (s, 18 H) ppm. ^{13}C NMR (101 MHz, $CDCl_3$): δ = 155.4, 139.4, 137.2, 136.1, 129.7, 127.1, 125.9, 124.6, 36.7, 31.3 ppm. IR (KBr): $\tilde{\nu}$ = 2961, 2861, 1951, 1924, 1822, 1709, 1612, 1533, 1479, 1436, 1405, 1383, 1298, 1261, 1184, 1115, 898, 879, 865, 763, 730, 584 cm^{-1}. HRMS: calcd. for $C_{36}H_{30}N_4$ $[M + H]^+$ 519.2543; found 519.2570.

2,13-Di-*tert*-butylbenzo[*i*]benzo[6′,7′]quinoxalino[2′,3′:9,10]-phenanthro[4,5-*abc*]phenazine (3db):[5a] Orange solid; yield 76 % (63 mg); m.p. >300 °C. ^1H NMR (400 MHz, $CDCl_3$): δ = 9.99 (s, 4 H), 9.38 (s, 4 H), 8.84 (m, 4 H), 7.94 (m, 4 H), 1.75 (s, 18 H) ppm. IR (KBr): $\tilde{\nu}$ = 2961, 1984, 1931, 1797, 1674, 1602, 1519, 1380, 1350, 1305, 1277, 1238, 1141, 1111, 1033, 960, 943, 905, 875, 831, 779, 754, 742, 668, 545 cm^{-1}. HRMS: calcd. for $C_{44}H_{34}N_4$ $[M + H]^+$ 619.2856; found 619.2877.

2,11-Di-*tert*-butyl-6,7,15,16-tetramethylquinoxalino[2′,3′:9,10]-phenanthro[4,5-*abc*]phenazine (3dc): Orange solid; yield 93 % (71 mg); m.p. >300 °C. ^1H NMR (400 MHz, $CDCl_3$): δ = 9.91 (s, 4 H), 8.52 (s, 4 H), 2.79 (s, 12 H), 1.72 (s, 18 H) ppm. ^{13}C NMR (101 MHz, $CDCl_3$): δ = 154.9, 149.4, 138.0, 136.5, 128.7, 126.4, 124.6, 124.4, 36.7, 31.3, 21.4 ppm. IR (KBr): $\tilde{\nu}$ = 2965, 2912, 2867, 2730, 2558, 2347, 1845, 1823, 1677, 1610, 1477, 1400, 1324, 1302, 1280, 1226, 1185, 1136, 1025, 1001, 899, 886, 865, 784, 732, 562 cm^{-1}. HRMS: calcd. for $C_{40}H_{38}N_4$ $[M + H]^+$ 575.3169; found 575.3190.

Dipyrido[3,2-*a*:2′,3′-*c*]phenazine (3ea): Orange solid; yield 94 % (63 mg); m.p. 248–250 °C (ref.[24] 246–247 °C). ^1H NMR (400 MHz, $CDCl_3$): δ = 9.67 (dd, J = 8.1, 1.6 Hz, 2 H), 9.29 (dd, J = 4.4, 1.5 Hz, 2 H), 8.38 (dd, J = 6.5, 3.4 Hz, 2 H), 7.95 (dd, J = 6.5, 3.4 Hz, 2 H), 7.82 (dd, J = 8.1, 4.4 Hz, 2 H) ppm. ^{13}C NMR (100 MHz, $CDCl_3$): δ = 152.8, 148.6, 142.7, 141.4, 134.0, 130.9, 129.8, 127.8, 124.4 ppm. HRMS: calcd. for $C_{14}H_{16}N_2O_3$ $[M + H]^+$ 283.0978; found 283.1003.

Benzo[*i*]dipyrido[3,2-*a*:2′,3′-*c*]phenazine (3eb):[25] Orange solid; yield 92 % (72 mg); m.p. 272–274 °C. ^1H NMR (400 MHz, $CDCl_3$): δ = 9.60 (d, J = 7.8 Hz, 2 H), 9.24 (d, J = 3.5 Hz, 2 H), 8.89 (s, 2 H), 8.18 (dd, J = 6.3, 2.9 Hz, 2 H), 7.78 (dd, J = 7.9, 4.4 Hz, 2 H), 7.62 (dd, J = 6.5, 2.9 Hz, 2 H) ppm. ^{13}C NMR (100 MHz, $CDCl_3$): δ = 152.7, 148.5, 142.0, 138.8, 134.6, 134.2, 128.7, 128.0, 127.9, 127.3, 124.5 ppm. HRMS: calcd. for $C_{22}H_{12}N_4$ $[M + H]^+$ 333.1135; found 333.1162.

11,12-Dimethyldipyrido[3,2-*a*:2′,3′-*c*]phenazine (3ec): White solid; yield 95 % (70 mg); m.p. 183–185 °C (ref.[26] 183 °C). ^1H NMR (400 MHz, $CDCl_3$): δ = 9.59 (dd, J = 8.1, 1.4 Hz, 2 H), 9.25 (dd, J = 4.3, 1.4 Hz, 2 H), 8.03 (s, 2 H), 7.78 (dd, J = 8.1, 4.4 Hz, 2 H), 2.58 (s, 6 H) ppm. ^{13}C NMR (100 MHz, $CDCl_3$): δ = 152.3, 148.3, 141.9, 141.7, 140.4, 133.6, 128.3, 127.9, 124.1, 20.8 ppm. HRMS: calcd. for $C_{20}H_{14}N_4$ $[M + H]^+$ 311.1291; found 311.1318.

Dipyrido[3,2-*a*:2′,3′-*c*]phenazine-11-carboxylic Acid (3ed):[27] White solid; yield 91 % (70 mg); m.p. >300 °C. ^1H NMR (400 MHz, $CDCl_3$): δ = 10.12 (t, J = 7.2 Hz, 2 H), 9.35–9.31 (m, 3 H), 8.69–8.67 (m, 1 H), 8.61 (d, J = 8.9 Hz, 1 H), 8.35 (td, J = 8.1, 5.2 Hz, 2 H) ppm. ^{13}C NMR (100 MHz, $CDCl_3$): δ = 170.3, 148.3, 147.7, 144.5, 141.6, 139.8, 139.3, 139.2, 139.1, 139.0, 138.9, 133.5, 131.2, 131.0, 130.0, 129.0, 128.9, 126.8, 126.8 ppm. HRMS: calcd. for $C_{19}H_{10}N_4O_2$ $[M + H]^+$ 327.0877; found 327.0893.

11,12-Dibromodipyrido[3,2-*a*:2′,3′-*c*]phenazine (3ee):[28] White solid; yield 96 % (100 mg); m.p. >300 °C. ^1H NMR (400 MHz, $CDCl_3$): δ = 10.04 (d, J = 7.5 Hz, 2 H), 9.32 (d, J = 4.0 Hz, 2 H), 8.83 (s, 2 H), 8.32 (dd, J = 8.2, 5.1 Hz, 2 H) ppm. ^{13}C NMR (100 MHz, $CDCl_3$): δ = 148.9, 142.4, 140.0, 139.9, 139.6, 133.8, 131.1, 129.9, 127.7 ppm. HRMS: calcd. for $C_{18}H_8Br_2N_4$ $[M + H]^+$ 440.9169; found 440.9193.

11,11′-Bidipyrido[3,2-*a*:2′,3′-*c*]phenazine (3eg):[29] Pale yellow solid; yield 88 % (58 mg); m.p. >300 °C. ^1H NMR (400 MHz, $CDCl_3$): δ = 10.23 (d, J = 7.2 Hz, 4 H), 9.34 (s, 4 H), 9.06 (s, 2 H), 8.79 (d, J = 8.8 Hz, 2 H), 8.72 (d, J = 8.8 Hz, 2 H), 8.38 (s, 4 H) ppm. ^{13}C NMR (100 MHz, $CDCl_3$): δ = 148.7, 148.5, 143.9, 143.7, 143.6, 140.6, 140.4, 139.8, 139.7, 139.6, 139.3, 133.0, 131.4, 130.5, 130.4, 128.7, 128.0, 128.0 ppm. HRMS: calcd. for $C_{36}H_{18}N_8$ $[M + H]^+$ 563.1727; found 563.1722.

Tribenzo[*a*,*c*,*i*]phenazine (3fb): Yellow solid; yield 96 % (76 mg); m.p. 291–293 °C (ref.[25] m.p. 293–294 °C). ^1H NMR (400 MHz, $CDCl_3$): δ = 9.25 (d, J = 7.9 Hz, 2 H), 9.10 (s, 2 H), 8.51 (d, J = 8.0 Hz, 2 H), 8.25–8.24 (m, 2 H), 7.95 (t, J = 7.1 Hz, 2 H), 7.84–7.77 (m, 4 H) ppm. ^{13}C NMR (100 MHz, $CDCl_3$): δ = 140.2, 136.3, 135.2, 133.8, 131.9, 130.5, 130.3, 129.0, 127.3, 124.5, 124.3, 124.2 ppm. HRMS: calcd. for $C_{24}H_{14}N_2$ $[M + H]^+$ 331.1230; found 331.1233.

11,12-Dimethyldibenzo[*a*,*c*]phenazine (3fc):[30] Pale yellow solid; yield 96 % (71 mg); m.p. 280–282 °C. ^1H NMR (400 MHz, $CDCl_3$): δ =

9.20 (dd, J = 8.2, 0.9 Hz, 2 H), 8.60 (d, J = 8.2 Hz, 2 H), 8.33 (s, 2 H), 7.97–7.93 (m, 2 H), 7.86 (t, J = 7.6 Hz, 2 H), 2.69 (s, 6 H) ppm. ^{13}C NMR (100 MHz, $CDCl_3$): δ = 148.3, 138.1, 135.6, 134.1, 133.2, 129.9, 126.3, 124.3, 124.2, 124.1, 21.1 ppm. HRMS: calcd. for $C_{14}H_{16}N_2O_3$ $[M + H]^+$ 309.1386; found 309.1368.

11,12-Dibromodibenzo[*a*,*c*]phenazine (3fe):[31] Pale yellow solid; yield 96 % (101 mg); m.p. 278–280 °C. ^{1}H NMR (400 MHz, $CDCl_3$): δ = 9.33 (d, J = 7.6 Hz, 2 H), 8.65 (s, 2 H), 8.57 (d, J = 8.0 Hz, 2 H), 7.85 (t, J = 7.4 Hz, 2 H), 7.77 (t, J = 7.3 Hz, 2 H) ppm. ^{13}C NMR (100 MHz, $CDCl_3$): δ = 143.6, 141.4, 133.5, 132.6, 131.2, 130.0, 128.4, 126.7, 126.5, 123.3 ppm. HRMS: calcd. for $C_{20}H_{10}Br_2N_2$ $[M + H]^+$ 436.9283; found 436.9233.

2,2′,3,3′-Tetraphenyl-6,6′-biquinoxaline (3gg): Pale yellow solid; yield 96 % (66 mg); m.p. >300 °C (ref.[32] >300 °C). ^{1}H NMR (400 MHz, $CDCl_3$): δ = 8.62 (s, 2 H), 8.35 (d, J = 8.4 Hz, 2 H), 8.26 (d, J = 8.2 Hz, 2 H), 7.58 (d, J = 6.0 Hz, 4 H), 7.38 (d, J = 6.5 Hz, 10 H) ppm. ^{13}C NMR (100 MHz, $CDCl_3$): δ = 154.4, 153.9, 141.7, 141.4, 141.2, 139.2, 130.2, 130.1, 129.7, 129.2, 128.5, 127.7 ppm. HRMS: calcd. for $C_{40}H_{26}N_4$ $[M + H]^+$ 563.2230; found 563.2244.

2,3,7,8-Tetraphenylpyrazino[2,3-*g*]quinoxaline (3gh):[33] Yellow solid; yield 90 % (50 mg); m.p. 280–282 °C. ^{1}H NMR (400 MHz, $CDCl_3$): δ = 9.03 (s, 2 H), 7.63 (d, J = 6.7 Hz, 8 H), 7.45–7.38 (m, 12 H) ppm. ^{13}C NMR (100 MHz, $CDCl_3$): δ = 155.6, 140.7, 139.1, 130.3, 129.7, 129.1, 128.6 ppm. HRMS: calcd. for $C_{34}H_{22}N_4$ $[M + H]^+$ 487.1917; found 487.1947.

Fluorescence Quantum Yield Determination: For fluorescence quantum yield determination, quinine sulfate[34] was used as the standard (Φ_{FI} = 0.577 in 0.1 N H_2SO_4, the irradiation wavelength was 350 nm). In a typical measurement, heteroacene stock solution (20 μL, 2.5×10^{-3} M in dichloromethane) was added to solvent (2.5 mL). Fluorescence wavelengths from 385 to 650 nm were considered for the calculation:

$$\frac{\varphi_1}{\varphi_2} = \frac{A_2 {n_1}^2 \alpha_1}{A_1 {n_2}^2 \alpha_2}$$

Here, φ = quantum yield, A = absorbance at a given wavelength (350 nm), n = refractive index, and α = the area under the fluorescence spectrum. Indices 1 and 2 designate the sample and standard, respectively.

X-ray Crystallography: The single-crystal X-ray diffraction data were collected at room temperature with a Bruker-SMART-APEX II D8 diffractometer with Mo-K_α (λ = 0.71073 Å) radiation. CCDC 1437948 (for **3ac**), 1437949 (for **3ae**), 1437950 (for **3ba**), and 1437951 (for **3cf**) contain the supplementary crystallographic data for this paper. These data can be obtained free of charge from The Cambridge Crystallographic Data Centre.

Supporting Information (see footnote on the first page of this article): experimental methods, spectroscopic investigations, synthetic procedure, characterization data, and spectra.

Acknowledgments

The authors are thankful to the Department of Science and Technology (DST), New Delhi for financial support (grant numbers INT/FINLAND/P-06 and SR/S1/IC-59/2010). P. K. S. is thankful to the University Grants Commission (UGC), New Delhi for a fellowship. The Academy of Finland (grants 263256 and 265328 to K. R.) and the University of Jyvaskyla, Finland are also gratefully acknowledged for financial support.

Keywords: Synthetic methods · Mechanochemistry · Solvent-free synthesis · Fused-ring systems · Nitrogen heterocycles · Polycycles

[1] a) M. Watanabe, K.-Y. Chen, Y. J. Chang, T. J. Chow, *Acc. Chem. Res.* **2013**, *46*, 1606–1615; b) H. Usta, A. Facchetti, T. J. Marks, *Acc. Chem. Res.* **2011**, *44*, 501–510; c) J. E. Anthony, *Angew. Chem. Int. Ed.* **2008**, *47*, 452–483; *Angew. Chem.* **2008**, *120*, 460; d) W. Jiang, Y. Li, Z. Wang, *Chem. Soc. Rev.* **2013**, *42*, 6113–6127; e) M. Randić, *Chem. Rev.* **2003**, *103*, 3449–3606.
[2] Y. Ruiz-Morales, *J. Phys. Chem. A* **2002**, *106*, 11283–11308.
[3] W. Yue, S. L. Suraru, D. Bialas, M. Muller, F. Wurthner, *Angew. Chem. Int. Ed.* **2014**, *53*, 6159–6162; *Angew. Chem.* **2014**, *126*, 6273.
[4] a) L. Qiu, X. Zhuang, N. Zhao, X. Wang, Z. An, Z. Lan, X. Wan, *Chem. Commun.* **2014**, *50*, 3324–3327; b) A. Mateo-Alonso, N. Kulisic, G. Valenti, M. Marcaccio, F. Paolucci, M. Prato, *Chem. Asian J.* **2010**, *5*, 482–485.
[5] a) N. Kulisic, S. More, A. Mateo-Alonso, *Chem. Commun.* **2011**, *47*, 514–516; b) A. Mateo-Alonso, *Chem. Soc. Rev.* **2014**, *43*, 6311–6324.
[6] B. Kohl, F. Rominger, M. Mastalerz, *Org. Lett.* **2014**, *16*, 704–707.
[7] a) R. B. N. Baig, R. S. Varma, *Chem. Soc. Rev.* **2012**, *41*, 1559–1584; b) S. Ley, M. O'Brien, R. Denton, *Synthesis* **2011**, 1157–1192.
[8] a) A. Stolle, T. Szuppa, S. E. S. Leonhardt, B. Ondruschka, *Chem. Soc. Rev.* **2011**, *40*, 2317–2329; b) G.-W. Wang, *Chem. Soc. Rev.* **2013**, *42*, 7668–7700.
[9] a) J. G. Hernández, C. G. Avila-Ortiz, E. Juaristi, in: *Comprehensive Organic Synthesis II* (Ed.: P. Knochel), 2nd ed., Elsevier, Amsterdam, The Netherlands, **2014**, p. 287–314; b) L. Takacs, *Chem. Soc. Rev.* **2013**, *42*, 7649–7659; c) S. L. James, T. Friscic, *Chem. Soc. Rev.* **2013**, *42*, 7494–7496; d) S. L. James, C. J. Adams, C. Bolm, D. Braga, P. Collier, T. Friscic, F. Grepioni, K. D. M. Harris, G. Hyett, W. Jones, A. Krebs, J. Mack, L. Maini, A. G. Orpen, I. P. Parkin, W. C. Shearouse, J. W. Steed, D. C. Waddell, *Chem. Soc. Rev.* **2012**, *41*, 413–447.
[10] S. Maiti, P. Mal, *Synth. Commun.* **2014**, *44*, 3461–3469.
[11] a) P. K. Sahoo, A. Bose, P. Mal, *Eur. J. Org. Chem.* **2015**, 6994–6998; b) T. K. Achar, P. Mal, *J. Org. Chem.* **2015**, *80*, 666–672; c) A. Bose, P. Mal, *Tetrahedron Lett.* **2014**, *55*, 2154–2156; d) T. K. Achar, S. Maiti, P. Mal, *RSC Adv.* **2014**, *4*, 12834–12839.
[12] C. Giri, P. K. Sahoo, R. Puttreddy, K. Rissanen, P. Mal, *Chem. Eur. J.* **2015**, *21*, 6390–6393.
[13] a) L. Carlier, M. Baron, A. Chamayou, G. Couarraze, *Tetrahedron Lett.* **2011**, *52*, 4686–4689; b) S. Paul, B. Basu, *Tetrahedron Lett.* **2011**, *52*, 6597–6602.
[14] J. Hu, D. Zhang, F. W. Harris, *J. Org. Chem.* **2005**, *70*, 707–708.
[15] A. Mateo-Alonso, N. Kulisic, G. Valenti, M. Marcaccio, F. Paolucci, M. Prato, *Chem. Asian J.* **2010**, *5*, 482–485.
[16] A. Mateo-Alonso, C. Ehli, K. H. Chen, D. M. Guldi, M. Prato, *J. Phys. Chem. A* **2007**, *111*, 12669–12673.
[17] A. Mateo-Alonso, N. Kulisic, G. Valenti, M. Marcaccio, F. Paolucci, M. Prato, *Chem. Asian J.* **2010**, *5*, 482–485.
[18] J. Fleischhauer, S. Zahn, R. Beckert, U.-W. Grummt, E. Birckner, H. Görls, *Chem. Eur. J.* **2012**, *18*, 4549–4557.
[19] Y. Wu, Z. Yin, J. Xiao, Y. Liu, F. Wei, K. J. Tan, C. Kloc, L. Huang, Q. Yan, F. Hu, H. Zhang, Q. Zhang, *ACS Appl. Mater. Interfaces* **2012**, *4*, 1883–1886.
[20] U. H. F. Bunz, *Chem. Eur. J.* **2009**, *15*, 6780–6789.
[21] F. G. Oberender, J. A. Dixon, *J. Org. Chem.* **1959**, *24*, 1226–1229.
[22] B. Wex, A. a. O. El-Ballouli, A. Vanvooren, U. Zschieschang, H. Klauk, J. A. Krause, J. Cornil, B. R. Kaafarani, *J. Mol. Struct.* **2015**, *1093*, 144–149.
[23] T. Yamato, M. Fujimoto, A. Miyazawa, K. Matsuo, *J. Chem. Soc. Perkin Trans. 1* **1997**, 1201–1208.
[24] F. Ferretti, E. Gallo, F. Ragaini, *J. Organomet. Chem.* **2014**, *771*, 59–67.
[25] W. Guo, B. J. Engelman, T. L. Haywood, N. B. Blok, D. S. Beaudoin, S. O. Obare, *Talanta* **2011**, *87*, 276–283.
[26] A. Kleineweischede, J. Mattay, *Eur. J. Org. Chem.* **2006**, 947–957.
[27] A. J. McConnell, M. H. Lim, E. D. Olmon, H. Song, E. E. Dervan, J. K. Barton, *Inorg. Chem.* **2012**, *51*, 12511–12520.
[28] B. Schafer, H. Gorls, M. Presselt, M. Schmitt, J. Popp, W. Henry, J. G. Vos, S. Rau, *Dalton Trans.* **2006**, 2225–2231.
[29] A. K. Bilakhiya, B. Tyagi, P. Paul, P. Natarajan, *Inorg. Chem.* **2002**, *41*, 3830–3842.
[30] S. M. Baghbanian, *Chin. Chem. Lett.* **2015**, *26*, 1113–1116.

[31] A. Putta, J. D. Mottishaw, Z. Wang, H. Sun, *Cryst. Growth Des.* **2014**, *14*, 350–356.
[32] M. Lian, Q. Li, Y. Zhu, G. Yin, A. Wu, *Tetrahedron* **2012**, *68*, 9598–9605.
[33] H. Takeshita, A. Mori, T. Nagao, T. Nagamura, *Chem. Lett.* **1989**, *18*, 1719–1722.
[34] J. R. Lakowicz, *Principles of Fluorescence Spectroscopy*, Springer, New York, **2006**, p. 27–61.

Received: January 4, 2016
Published Online: January 19, 2016

